

## Watching bismuth nanowires grow

Jinhee Ham,<sup>1</sup> Wooyoung Shim,<sup>1,2</sup> Do Hyun Kim,<sup>3</sup> Kyu Hwan Oh,<sup>3</sup> Peter W. Voorhees,<sup>2,a)</sup> and Wooyoung Lee<sup>1,a)</sup>

<sup>1</sup>Department of Materials Science and Engineering, Yonsei University, 134 Shinchon, Seoul 120-749, Republic of Korea

<sup>2</sup>Department of Materials Science and Engineering, Northwestern University, Evanston, Illinois 60208, USA

<sup>3</sup>Department of Materials Science and Engineering, Seoul National University, Seoul 151-744, Republic of Korea

(Received 6 October 2010; accepted 2 December 2010; published online 25 January 2011)

We report real-time high temperature scanning electron microscopy observations of the growth of bismuth nanowires via the on-film formation of nanowires (OFF-ON) method. These observations provide experimental evidence that thermally induced-stress on a Bi film is the driving force for the growth of Bi nanowires with high aspect ratios, uniform diameter, and high-quality crystallinity. Our results show that immobile grain boundaries in the Bi film are required for the growth of nanowires so that grain broadening resulting in hillock formation can be prevented. This study not only provides an understanding of the underlying mechanism, but also affords a strategy for facilitating nanowire growth by OFF-ON. © 2011 American Institute of Physics. [doi:10.1063/1.3535956]

During the past 50 years, the formation of metal whiskers on the surface of electrical components has been an issue of great technological concern that could threaten electronic device reliability. The majority of failure includes commercial satellites,<sup>1</sup> military,<sup>2</sup> medical,<sup>3</sup> and industrial devices<sup>4</sup> which result in costly repairs. Simultaneously, attempts to understand the mechanism of spontaneous growth and formation of metal whiskers in an effort to develop a practical strategy to prevent the whisker formation have been developed.<sup>5–8</sup> Due to the complex dependence of the whisker formation on the thermodynamics and kinetics of nucleation and growth, however, the mechanism is still under investigation.

On the scientific side, however, whiskers are “nearly” perfect single crystal structures (diameters of  $\sim 1\text{--}10\ \mu\text{m}$  and lengths up to several millimeters) that are potentially suitable for exploring material and size-dependent properties. In particular, the nanometer length scale where such properties can be quite different from the bulk is more desirable for this context. Recently, we have developed a methodology, termed the on-film formation of nanowires (OFF-ON), to grow high quality, single-crystalline nanowires in a similar fashion with that of a whisker formation,<sup>9,10</sup> which presumably utilizes thermally induced compressive stress within a polycrystalline thin film. OFF-ON combines the concepts and advantages of simple thin film deposition with whisker formation that produces highly crystalline one-dimensional nanomaterials. Unlike other whisker formation method, it is worth noting that OFF-ON offers significant advantages of (1) providing tunability where one can control the nanowire diameter, i.e., Bi, as small as a few tens of nanometers<sup>9</sup> and (2) enabling the synthesis of thermodynamically stable compound semiconductors, i.e.,  $\text{Bi}_2\text{Te}_3$ ,<sup>10</sup> which uses conventional whisker formation as a positive tool to make functional materials for device applications. The utility of this method has been demonstrated in the context of oscillatory<sup>11</sup> and nonoscillatory magnetoresistance measurements<sup>12</sup> in Bi

nanowires that provide evidence for the high-quality crystalline of the nanowires grown by OFF-ON. In fact, the demand for OFF-ON become increasingly important as bismuth and its alloys have emerged as attractive candidates for high-efficiency thermoelectric materials ( $\text{Bi}$ ,<sup>13</sup>  $\text{Bi}_2\text{Te}_3$ ,<sup>14</sup>  $\text{Bi-Sb}$ ) (Ref. 15) and topological insulators ( $\text{Bi}$ ,<sup>16</sup>  $\text{Bi}_2\text{Te}_3$ ,<sup>17</sup>  $\text{Bi}_2\text{Se}_3$ ,<sup>18</sup>  $\text{Bi}_x\text{Sb}_{1-x}$ ) (Ref. 19) where the crystallinity of the wires needs to be exceptionally high. In this regard, an attempt to identify the growth mechanism which expands the range of materials readily available for synthesis by OFF-ON must be investigated. Herein, we report the direct observation of Bi nanowire growth that allows one to clarify the growth mechanism of OFF-ON as a tool for producing high-quality nanowires. The mechanism is found to be thermal stress-induced mass flow along immobile grain boundaries in the polycrystalline film. Fast growth of nanowire having uniform diameters with aspect ratios exceeding  $10^3$  was observed; these materials ultimately can be used as building blocks for one-dimensional nanoscale devices.

In a typical experiment, a Bi thin film was deposited onto a thermally oxidized Si(100) substrate at a rate of  $\sim 30\ \text{\AA}/\text{s}$  using an ultrahigh vacuum radio frequency sputtering system and heated up to  $270\ ^\circ\text{C}$ , one degree below the melting point of Bi. More experimental details have been presented in previous work.<sup>9</sup> Figure 1(a) shows a series of scanning electron microscope (SEM) images of a Bi nanowire that grows with time at various temperatures. By heating the Bi-deposited Si/SiO<sub>2</sub> sample *in situ*, it was possible to observe the resulting nanowire evolution in real time and at high spatial resolution. Here, the length of the nanowire was found to be 12, 20, 25, 41, 66, and  $80\ \mu\text{m}$  with increasing annealing temperatures and time corresponding to 90 (30 min), 95 (60 min), 100 (90 min), 115 (125 min), 130 (160 min), and  $160\ ^\circ\text{C}$  (200 min), respectively. The average growth rate is approximately  $4.6\ \text{nm}/\text{s}$  in these images and can be up to  $27.7\ \text{nm}/\text{s}$ , which will be discussed later. These direct observations provide experimental evidence that clarify the driving force for Bi nanowire growth; compressive stress is generated by a mismatch between the thermal expansion of the Bi thin film ( $13.4 \times 10^{-6}/^\circ\text{C}$ ) and SiO<sub>2</sub>/Si [ $(0.5 \times 10^{-6}/^\circ\text{C})/(2.4 \times 10^{-6}/^\circ\text{C})$ ] when heat is applied.

<sup>a)</sup>Authors to whom correspondence should be addressed. Electronic addresses: wooyoung@yonsei.ac.kr and p-voorhees@northwestern.edu.

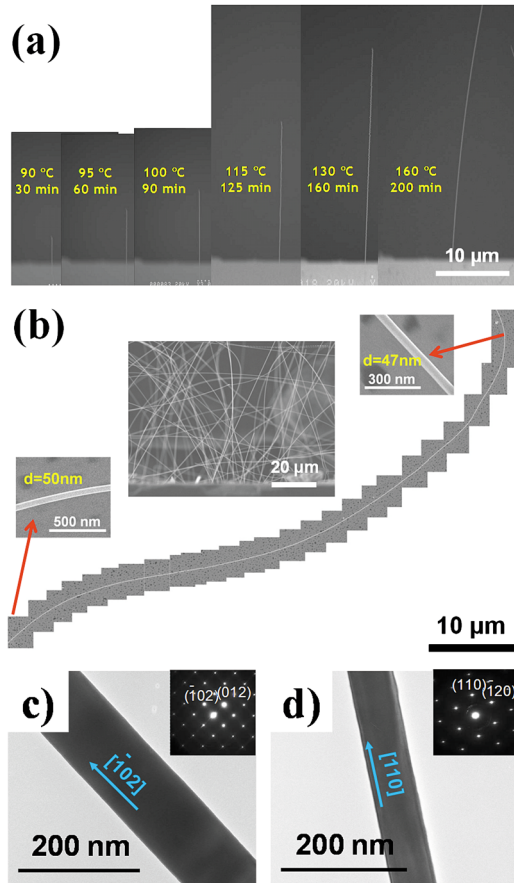


FIG. 1. (Color online) Growth and structural characterization of single-crystalline Bi nanowires. (a) A series of six SEM images of a Bi nanowire grown by OFF-ON with time at various temperatures. (b) A series of 27 SEM images of a  $77\ \mu\text{m}$  long Bi nanowire transferred onto a  $\text{SiO}_2/\text{Si}$  substrate. The inset (top right and bottom left) show SEM images of starting and end segments of this NW. The inset (middle) shows SEM image of as-grown ultralong Bi nanowires. A low-magnification TEM image of Bi nanowires with the growth axis of (c)  $[\bar{1}02]$  and (d)  $[110]$ . Inset (top right) shows the electron diffraction pattern of the corresponding nanowire.

The Bi film expands when it is annealed, while the substrate restricts expansion, putting the Bi film under compressive stress. Importantly, no change in diameter was observed as the nanowire grew as shown in Fig. 1(a), indicating that the Bi nanowire grew through continuous addition to its base, as opposed to possible thermal evaporation from the Bi film at high temperatures. Quantitative analysis of the uniformity in diameter is more visualized in a series of 27 SEM images taken along the length of a representative ultralong Bi nanowire in Fig. 1(b). The length of this nanowire is  $77\ \mu\text{m}$  and the diameter does not change significantly with starting and end diameters of approximately 50 and 47 nm, respectively. The entire Bi nanowire can also be readily seen in dark-field optical microscopy images that make them more accessible to conventional device fabrication processes. Therefore, it is especially important to point out that OFF-ON retains many of the advantages of whisker formation, namely, fast growth rate with uniformity in diameter, as well as high-quality crystal with control over size. In this study, Bi nanowires were single crystals as characterized by transmission electron microscopy (TEM) and shown in Figs. 1(c) and 1(d). The growth axes were found to be  $[\bar{1}02]$  and  $[110]$ .

In general, whisker and hillock formation occur on the same surface. Figure 2(a) shows a SEM image of Bi thin film

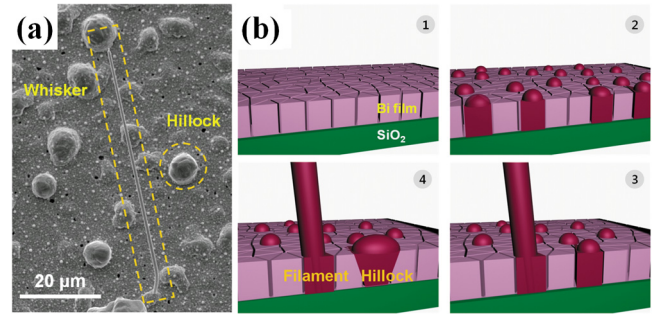


FIG. 2. (Color online) Coexistence of whisker and hillock. (a) SEM image of Bi whisker and hillocks on a surface of Bi thin film. (b) Schematics of different response of surface grains to the biaxial stress depending on the mobility of the grain boundary.

surface after annealing for 10 h at  $270\ ^\circ\text{C}$  where the temperature is close to the melting point of Bi ( $271.3\ ^\circ\text{C}$ ). A nanowire whisker and spherical hillocks are evident on the surface of a Bi thin film. The hillocks are larger ( $7.4\ \mu\text{m}$  in width) than the whisker diameter ( $770\ \text{nm}$  in diameter). According to previous studies, the motion of grain boundaries is largely responsible for the growth of whiskers and hillocks.<sup>5,20</sup> The high mobility of grain boundaries during migration results in broad hillocks on a surface, whereas low mobility or pinned boundaries promotes whisker formation by maintaining a laterally small grain where atom flux accumulates. In addition, it has been reported that the diameter of Bi nanowires was strongly coupled to the grain size of a film; the diameter of nanowires grown on a film decreases as the grain size of a film decreases.<sup>9</sup> By combining the role of grain boundary motion with the correlation between nanowire diameter and the grain size of a film, a proper model for the growth of Bi whiskers and hillocks is shown in Fig. 2(b). One grain with a mobile grain boundary can be broadened laterally by grain boundary migration as it is pushed upward [Fig. 2(b)], while the other grain broadening can be hindered with pinned grain boundaries that promote the nanowire formation.

To obtain a better understanding of the growth mechanism, a Bi nanowire of  $150\ \text{nm}$  in diameter grown on a Bi thin film was selected [Fig. 3(a)] for a cross-sectional sample [Fig. 3(b)] prepared by a focused ion beam (FIB)/field emission-SEM dual-beam system (FEI, Nova nanoLab200, USA). To prevent damage from the  $\text{Ga}^+$  ion beam during the TEM sampling process, electron beam-induced Pt deposition, followed by ion beam inducing Pt deposition were performed all around the nanowire and substrate [see Fig. 3(b)].

Figures 3(c) and 3(d) show the cross-sectional dark-field TEM images, grown the Bi nanowire on an annealed Bi film. The low magnification TEM image [Fig. 3(c)] shows that the Bi thin film is polycrystalline and consists of many columnar grains, and that the Bi nanowire is a single crystal. From the analysis of corresponding electron diffraction patterns [inset of Fig. 3(c)] as indicated, the growth direction of the Bi nanowire is  $[110]$ . These results provide insights into the mechanisms of Bi-wire growth. Using the measurements of the wire length, times, and temperatures shown in Fig. 1(a), it is clear that the average velocity measured over a given time interval at a certain temperature is relatively uncorrelated with temperature, for example, the average velocity decreases as the temperature is increased from  $90\ ^\circ\text{C}$ , and then suddenly increases at  $115\ ^\circ\text{C}$ , and then decreases on going

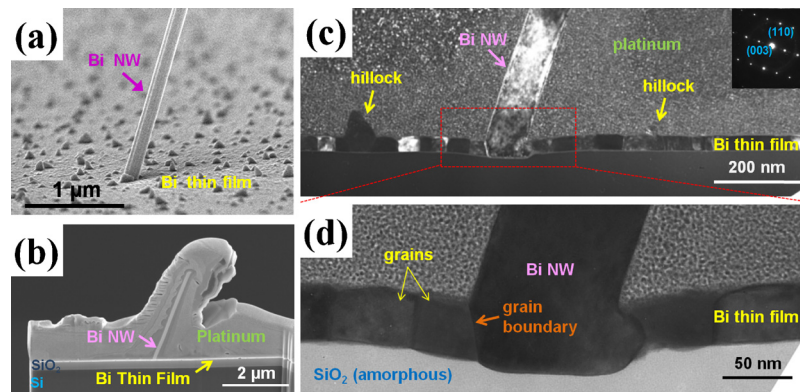


FIG. 3. (Color online) SEM and TEM study of the cross-section of a Bi nanowire-Bi thin film. (a) Representative SEM image of an individual Bi nanowire grown on a Bi thin film. (b) The cross-sectional Bi nanowire prepared by a FIB/FE-SEM dual beam system. The cross-section was sliced down to a thickness of 60 nm and lifted by a manipulating probe (Model 100.7™, Omniprobe, USA). Then the thickness of the nanowire was reduced to 5–60 nm using FIB milling for TEM analysis. To prevent the formation of an amorphous layer on the surface caused by the Ga<sup>+</sup> ion beam-induced damage, the sample was finally cleaned under low energy conditions (accelerating voltage of 5 kV and ion current of 70 pA). (c) High resolution TEM image of the cross-sectional Bi nanowire grown on a Bi thin film. (d) Magnified image of the Bi nanowire grown at the grain of the Bi thin film.

from 130 to 160 °C. A likely explanation for this is that the instantaneous growth rate at a given temperature is not constant, as observed experimentally in other systems.<sup>6,7,21</sup> Complex competition between driving force and kinetics, which determines the growth rate, may account for nonconstant growth rate of the Bi nanowires but the exact mechanism regarding the temperature dependence of the growth rate remains unclear. Figure 3(d) shows that the SiO<sub>2</sub> substrate beneath the wire is nonplanar, but the thickness of the film in this region is unchanged. This indicates that the local stress in this area is sufficient to induce diffusion of SiO<sub>2</sub> away from this region. However, on careful inspection of Fig. 3(d), it is clear that the degree of nonplanarity is larger on the left side of the wire than the right. This may be due to grain boundary sliding of the grain, denoted by the arrow, since this boundary is inclined with respect to the applied stress. This grain boundary sliding process concentrates the stress in this region, leading to the stress in the SiO<sub>2</sub> layer. By contrast the grain boundary on the right side cannot slide since it is perpendicular to the substrate. This sliding process reduces the stress that drives wire growth. If the grain boundary-sliding rate was not constant this would introduce a time-changing stress that would lead to the nonconstant instantaneous growth rate mentioned above. Finally, the growth direction of the wires is unrelated to the orientation of the grain boundaries at the root of the wire, unlike Bi<sub>2</sub>Te<sub>3</sub> wires.<sup>10</sup> As shown in Fig. 3(d), the (110) planes are inclined with respect to the SiO<sub>2</sub> substrate. This implies that growth occurs not one (110) plane at a time, but by atom attachment where the ends of the (110) planes contact the grain boundary and substrate. This is also why, although there is clear preferred growth direction of the wires, the angle of the wires with respect to the substrate is not fixed [see Fig. 1(b)]. Finally, Fig. 3(c) shows hillocks as well. These also form in response to the compressive stress, but since the hillocks are bounded by mobile grain boundaries, lateral motion of the boundary is significant and a wire does not form.<sup>5,20</sup>

Moving forward, an investigation that consists of controlling various spatial growth direction of nanowires and making functional heterostructures such as core-shell and superlattice nanowires will be needed to fully exploit the capabilities afforded by this technique.

This work was supported by Priority Research Centers Program (Grant No. 2009-0093823) through the National Research Foundation of Korea (NRF), by NRF through National Core Research Center for Nanomedical Technology (Grant No. R15-2004-024-00000-0), and by a grant from “Center for Nanostructured Materials Technology” under “21st Century Frontier R&D Programs” of the Ministry of Education, Science and Technology. J.H. and W.S. contributed equally to this work.

<sup>1</sup>S. Silverstein, Space News, 17–23 August 1998.

<sup>2</sup>U.S. Missile Program, J. Richardson, and B. Lasley, Proceedings of the 1992 Government Microcircuit Applications Conference, 10–12 November 1992, Vol. 18, p. 119.

<sup>3</sup>J. Downs, Met. Finish. **August**, 23 (1994).

<sup>4</sup>C. Stevens, IEEE Boston Reliability Chapter 38th Annual Spring Reliability Symposium, 16 May 2001.

<sup>5</sup>W. Boettinger, C. Johnson, L. Bendersky, K. Moon, M. Williams, and G. Stafford, *Acta Mater.* **53**, 5033 (2005).

<sup>6</sup>K. Tu, C. Chen, and A. Wu, *J. Mater. Sci.: Mater. Electron.* **18**, 269 (2007).

<sup>7</sup>M. Sobiech, U. Welzel, E. Mittemeijer, W. Hugel, and A. Seekamp, *Appl. Phys. Lett.* **93**, 011906 (2008).

<sup>8</sup>M. Sobiech, M. Wohlschlogel, U. Welzel, E. Mittemeijer, W. Hugel, A. Seekamp, W. Liu, and G. Ice, *Appl. Phys. Lett.* **94**, 221901 (2009).

<sup>9</sup>W. Shim, J. Ham, K. Lee, W. Jeung, M. Johnson, and W. Lee, *Nano Lett.* **9**, 18 (2009).

<sup>10</sup>J. Ham, W. Shim, D. Kim, S. Lee, J. Roh, S. Sohn, K. Oh, P. Voorhees, and W. Lee, *Nano Lett.* **9**, 2867 (2009).

<sup>11</sup>W. Shim, J. Ham, J. Kim, and W. Lee, *Appl. Phys. Lett.* **95**, 232107 (2009).

<sup>12</sup>W. Shim, D. Kim, K. I. Lee, K. J. Jeon, J. Ham, J. Chang, S. H. Han, W. Y. Jeung, M. Johnson, and W. Lee, *J. Appl. Phys.* **104**, 073715 (2008).

<sup>13</sup>A. Boukai, K. Xe, and J. R. Heath, *Adv. Mater. (Weinheim, Ger.)* **18**, 864 (2006).

<sup>14</sup>J. Zhou, C. Jin, J. H. Seol, X. Li, and L. Shi, *Appl. Phys. Lett.* **87**, 133109 (2005).

<sup>15</sup>W. Yim and A. Amith, *Solid-State Electron.* **15**, 1141 (1972).

<sup>16</sup>J. Moore, *Nat. Phys.* **5**, 378 (2009).

<sup>17</sup>D. Kong, J. C. Randal, H. Peng, J. J. Cha, S. Meister, K. Lai, Y. Chen, Z. Shen, H. C. Mran, and Y. Cui, *Nano Lett.* **10**, 329 (2010).

<sup>18</sup>H. Peng, K. Lai, D. Kong, S. Meister, Y. Chen, X. Qi, S. Zhang, Z. Shen, and Y. Cui, *Nature Mater.* **9**, 225 (2009).

<sup>19</sup>H. Zhang, C. Liu, X. Qi, X. Dai, Z. Fang, and S. Zhang, *Nat. Phys.* **5**, 438 (2009).

<sup>20</sup>N. Jadhav, E. Buchovecky, E. Chason, and A. Bower, *J. Met.* **62**, 30 (2010).

<sup>21</sup>G. T. Galyon, *IEEE Trans. Electron. Packag. Manuf.* **28**, 94 (2005).